Experimental control of excitation flow produced by delayed pulses in a ladder of molecular levels

Ruth Garcia-Fernandez, Bruce W. Shore,[a] and Klaas Bergmann[b]
Fachbereich Physik der Universität, Erwin-Schrödinger-Strasse, 67653 Kaiserslautern, Germany

Aigars Ekers[c]
Institute of Atomic Physics and Spectroscopy, University of Latvia, Raina Boulevard 19, LV-1586 Riga, Latvia

Leonid P. Yatsenko
Institute of Physics, National Academy of Science of Ukraine, Prospect Nauki 46, Kiev-39 03650, Ukraine

(Received 28 February 2006; accepted 17 April 2006; published online 5 July 2006)

We study a method for controlling the flow of excitation through decaying levels in a three-level ladder excitation scheme in Na_2 molecules. Like the stimulated Raman adiabatic passage (STIRAP), this method is based on the control of the evolution of adiabatic states by a suitable delayed interaction of the molecules with two radiation fields. However, unlike STIRAP, which transfers a population between two stable levels g and f via a decaying intermediate level e through the interaction of partially overlapping pulses (usually in a Λ linkage), here the final level f is not long lived. Therefore, the population reaching level f decays to other levels during the transfer process. Thus, rather than controlling the transfer *into* level f, we control the flow of the population *through* this level. In the present implementation a laser P couples a degenerate rovibrational level in the ground electronic state $X\ ^1\Sigma_g^+$, $v''=0$, $j''=7$ to the intermediate level $A\ ^1\Sigma_u^+$, $v'=10$, $J'=8$, which in turn is linked to the final level $5\ ^1\Sigma_g^+$, $v=10$, $J=9$ by a laser S, from which decay occurs to vibrational levels in the electronic A and X states. As in STIRAP, the maximum excitation flow through level f is observed when the P laser precedes the S laser. We study the influence of the laser parameters and discuss the consequences of the detection geometry on the measured signals. In addition to verifying the control of the flow of population through level f we present a procedure for the quantitative determination of the fraction κ_f of molecules initially in the ground level which is driven through the final level f. This calibration method is applicable for any stepwise excitation.
 [DOI: 10.1063/1.2203629]

I. INTRODUCTION

Preparation of atoms or molecules in well-defined quantum states is required in many branches in physics, such as atomic and molecular collisions,[1] control of chemical reactions,[2] quantum information processing,[3] and investigation of atoms and molecules in highly excited (Rydberg) states.[4] A single-photon excitation is often not practical for the excitation of atomic or molecular Rydberg states, either because the handling of the required short wavelength photons is inconvenient or because the transition dipole moment is too small. Therefore, it is often necessary to proceed with some form of multiple-step (or multiphoton) excitations. The simplest of these, considered here, is via two laser fields that resonantly link three degenerate levels (ground g, intermediate e, and final f) in a ladder linkage pattern of increasing energy $E_g<E_e<E_f$.

The theoretical treatment of lossy three-state excitation by near-resonant pulsed lasers, as underlies the present work, dates back many years ago (see for example Ref. 5). These discussions of adiabatic and nonadiabatic passages are applicable here.

In this work we expand on the results presented in Ref. 6 by providing a comparison of experimental results with numerical simulation studies and by discussing a calibration procedure to allow a quantification of the results. We present data that demonstrate the control of the population flow through the degenerate levels e and f by means of the delay between two laser pulses.[6] The coupling scheme is shown in Fig. 1. A laser P couples the g level to the intermediate level e, which in turn is coupled to the final level f by laser S.

It is straightforward to move population through level e alone by a single-photon excitation driven by the P field. However, few methods can accomplish a two-photon transfer with high probability. The technique presented earlier[6] for the preparation of molecules or atoms in highly excited levels has remarkable advantages over existing methods. In particular, it requires smaller intensities. Like the stimulated Raman adiabatic passage (STIRAP), it is robust against small-to-moderate variations of intensity. We here verify the success of this method quantitatively using a novel procedure for calibrating the population flow.

Several schemes that will move the population through

[a]Permanent address: 618 Escondido Cir., Livermore, CA 94550.
[b]Electronic mail: bergmann@rhrk.uni-kl.de
[c]Electronic mail: ekers@latnet.lv

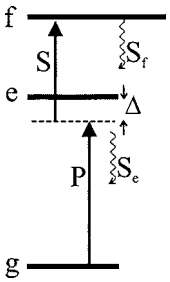

FIG. 1. The three-level ladder system. Laser P, possibly detuned by Δ, couples the initial and intermediate degenerate levels g and e, respectively. The latter level is coupled to the final level f by the laser S, properly detuned to maintain the two-photon resonance. The fluorescence from levels f and e leads to the detector signals S_f and S_e, respectively.

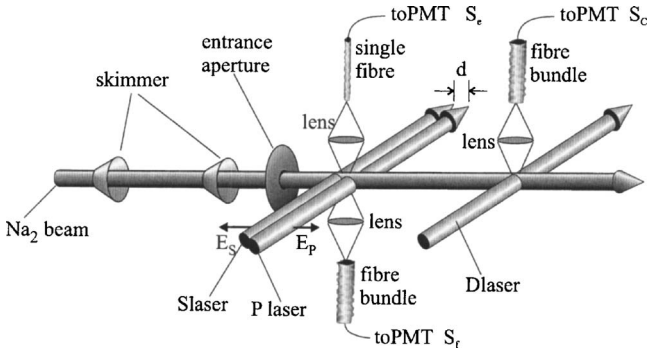

FIG. 2. Experimental setup showing the arrangement of the molecular beam, the laser beams (S, P, and D), and the detectors (S_f, S_e, and S_c). Short arrows show linear polarization directions for S and P beams.

level f alone can be imagined. The methods can be distinguished by the timing of the two fields (either simultaneous or delayed) and whether the frequencies, possibly detuned from the respective resonances, are fixed or swept through the resonance.[7] When the pulses act simultaneously at fixed frequencies and if both fields are resonant, with the time-integrated interaction strength suitably chosen, the sequence of pulses will move the population first into level e and then into level f. Damped one- and two-photon Rabi oscillations that produce population flow through levels e and f occur. With the use of monotonically varying detuning (a chirp), it is also possible to move the population effectively between two quantum states, via a chirped-frequency adiabatic passage. In either case, however, some populations inevitably flow out of level e.

We discuss an alternative procedure,[6] one in which it is possible to direct the flow of the population either completely through level e or through level f by adjusting the delay of the two pulses. When the molecules interact first with the P pulse, almost all the populations will decay through level e. If the pulses are applied simultaneously, some populations will decay through level f. However, if the S pulse arrives before the P pulse, almost all the populations will decay through level f. Thus, control of the pulse timing offers a means for controlling the population flow.

The STIRAP method[8] provides a high selectivity and efficiency, since it allows a complete population transfer to a unique target level. The linkages are such that the intermediate level e has a greater energy than do the initial and the final levels (a Λ linkage). The success of this method relies on the use of a pulse sequence wherein the S pulse (connecting levels e and f) precedes the P pulse (connecting g and e). This method has been widely studied, both in atomic and molecular systems, but mainly in the traditional Λ linkage. Prior to our previous work on this subject[6] there was one experimental work related to a STIRAP-like technique in a ladder configuration in atoms.[9] A numerical study of the same system appeared in Ref. 10. Results from further theoretical works will appear in Ref. 11.

There is one essential difference between driving population up a ladder and the usual STIRAP transfer process in a Λ system. In a ladder the final level decays on a time scale which is (much) shorter than the interaction time with the laser. Therefore, there exists no proper adiabatic dark state,[12] an adiabatic state that traps the population of the g-e-f level system despite the coupling to the radiation fields. Rather than considering the level population, we need to discuss the population flow through this level. The latter is represented by the time-integrated excitation probability, and not by the population transfer (which is ultimately zero). Maximizing the population flow through the upper level f is the most relevant goal for collision studies involving excited molecules. The benefit is particularly valuable if the collision process involves a barrier which prevents contributions from level e or if the outcome of the collision can be directly linked to level f, for instance, by energy balance.

II. EXPERIMENTAL SETUP

The experiments were performed in a supersonic beam of Na_2 molecules. The apparatus has been described in Sec. III of Ref. 13. Briefly, some 99% of the molecules were in the ground vibrational level $v''=0$; the distribution over the rotational levels had a maximum at $J''=7$. The number density of molecules was about 2×10^{10} cm^{-3} in the interaction zone with the laser radiation. The mean flow velocity of molecules in the beam was 1340 m/s, with a $1/e$ full width of the velocity distribution of 260 m/s. The molecular beam was collimated to a diameter of 3 mm, with a divergence angle ≈1°, resulting in a Doppler width of the molecular transitions of about 30 MHz when excited by radiation which propagates perpendicular to the molecular beam axis.

The molecular beam was crossed at right angles by three parallel cw laser beams (all Coherent Co., CR-699-21 dye lasers, with bandwidth $\Delta\nu_L \lesssim 1$ MHz) (see Fig. 2). The P and S lasers were linearly polarized parallel to the molecular beam axis. They were focused by means of a cylindrical lens, with the long axis perpendicular to the molecular beam axis. The focal position of the S beam relative to the P beam along the molecular beam axis was controlled by a micrometer screw-driven stepper motor. The adjustment of the beam waists and positions were monitored using a beam-profile measurement device (Dataray Beamscope-P7). A third laser beam D used for calibrating the efficiency of the process crossed the molecular beam downstream from the excitation zone. The fluorescence from the interaction zone with the S and P lasers was collected by two optical fiber bundles and detected by two photomultipliers equipped with filters that

allowed the separation of the fluorescence from levels e and f. The fluorescence signal induced by the D laser was also collected by an optical fiber and detected by a third photomultiplier further downstream.

III. EXPERIMENTAL RESULTS

We present in this section quantitative experimental results for the fraction of the initial level population which reaches the final level f. This fraction can be controlled through the power of the lasers, the detunings, and the spatial offset between the axes of the laser beams. The calibration procedure which puts the results on an absolute scale is discussed in Sec. IV.

The results of interest involve an excitation produced by P and S lasers and a fluorescence decay from the final level, as in the schematic sequence

$$g \overset{P}{\rightarrow} e \overset{S}{\rightarrow} f \rightsquigarrow S_f. \tag{1}$$

Decay occurs also from the intermediate level e. We detect the fluorescence from f as a signal S_f, and that from the excited level e as S_e; wavelength dependent filters discriminate between these two signals.

The signals S_n $(n=e,f)$ are proportional to the time integral of $P_n(t)$, which gives the probability of a molecule to be found in level n at time t, and to the decay rate Γ_n from level n. The parameter κ_f (see Sec. IV A 2), which gives the fraction of the molecules initially in the ground level g and that have decayed through level f, is given by

$$\kappa_f = \frac{\Gamma_f \int dt P_f(t)}{P_g(0)}. \tag{2}$$

A. Control through offset

Figure 3 shows a typical result for the averaged fraction $\bar{\kappa}_f$ (see Sec. IV A 3 below) of the initial level population driven to level f as a function of the displacement d between the axes of the P- and S-laser beams, when both lasers are resonant (full circles) and when the S and P lasers are detuned by $\Delta_P=200$ MHz and $\Delta_S=-200$ MHz (open circles) while maintaining the two-photon resonance $\Delta_P+\Delta_S=0$. Here we define detunings as $\Delta_P \equiv \omega_P-(E_e-E_g)/\hbar$ and $\Delta_S \equiv \omega_S-(E_f-E_e)/\hbar$. This experimental data has been displayed in an earlier work.[6] Now we put them on an absolute scale and add some numerical simulation. Unlike the signal from level f, the normalization of the signal from level e is not possible with the current experimental setup for reasons discussed in Sec. IV.

For these results the position of the S-laser beam remained unchanged, while the axis of the P-laser beam was moved with respect to the axis of the S-laser beam along the molecular beam axis. The powers of the P and S lasers were 400 and 390 mW, respectively. The P and S-laser beams were focused to a Gausian waist of 90 and 120 μm, respectively, with the long axis of 1.2 mm perpendicular to the molecular beam axis. For $d=0$ the axis of the S and P lasers coincided. For $d<0$ the molecules interacted with the S-laser field first. The signal shown in Fig. 3, exhibits the typical

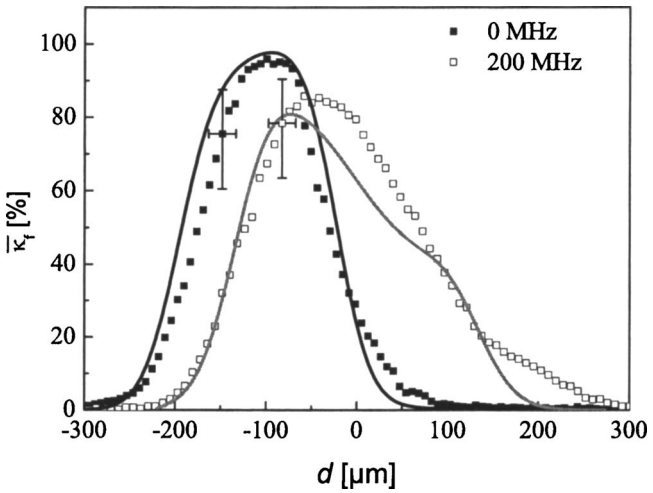

FIG. 3. Variation of the fraction $\bar{\kappa}_f$ of the initial population in level g, which is driven through level f, as a function of the displacement d between the axes of the S and P lasers. The full squares show results for $\Delta=0$ and the open squares for $\Delta=200$ MHz. Solid lines correspond to the numerical simulation. The indicated abscissa error bar takes into account the inaccuracy of the beam profiler measurement device, the micrometer positioning screw, and the control of the positions of the laser profile focus. The ordinate error bar takes into account inaccuracies in the determination of the calibration procedure (as specified in Sec. IV A 3).

signature of a STIRAP-type process. A maximum efficiency of about 95% is observed for $d<0$ (corresponding to a "counterintuitive" pulse sequence). Thus, for $d<0$ and for laser pulses with a sufficient overlap, the population flows almost entirely through the upper level. Of course, when there is no overlap or the P-laser field precedes the S field $d>0$, excitation flows almost entirely through the intermediate level e.

The population that flows through level f will decay to other levels, including level e. For our level scheme according to previous calculations,[14] a fraction of about $r=0.35$ of the molecules which are excited to level f will decay to level e. The population dynamics takes place during the relevant time interval that begins with the arrival of the P pulse and ends within $T_{\text{flow}} \sim \tau_f$, where $\tau_i=1/\Gamma_i$ is the total spontaneous emission rate from level i.[6] Since the lifetime τ_f is much shorter than the pulse duration, after spontaneous transitions from level f to level e the S-laser intensity is still large, while the P-laser intensity is small. Thus, the strong S laser will induce damped Rabi oscillations between levels e and f with a frequency that is much larger than the level decay rates $\Gamma_i=1/\tau_i$. In the limit of a very high Rabi frequency $\Omega \gg \Gamma_i$, the mean populations of the levels are equal. Then, the rate of the total population decay out of the system is $\Gamma_t=[(1-r)\Gamma_f+\Gamma_e]/2$, with the mean rate $dS_i/dt=(1/2)\Gamma_i \exp[-\Gamma_t t]$ of the spontaneous photon emission from level i (including spontaneous photons of the transition from f to e for the case $i=f$). Thus, the maximum number of spontaneous photons emitted from state f by a single molecule is $S_{f,\max}=1+r\Gamma_f/2\Gamma_t>1$. The maximum number of photons that can be emitted from level e is $S_{e,\max}=r\Gamma_e/\Gamma_t$. Under the conditions of the experiment we have $\Omega_S^2 \gtrsim \Gamma_e\Gamma_f$. Thus, the ratio τ_f/T of the spontaneous emission lifetime τ_f and the pulse duration $T \sim 70$ ns is not very small compared to unity, and therefore

the influence of the pump laser is also important. As a result, the observed $\bar{\kappa}_f$ would not increase by more than 10%, compared to the value expected for $r=0$. However, as explained in Sec. IV A 2, our calibration procedure is based on the measurement of fluorescence signals induced from the ground level g by the molecules that flowed through level f and decayed to the ground level g_2 (see Fig. 5). Therefore, cycling of the population between the f and e levels (induced by the S laser), accompanied by the emission of more than one photon, does not affect the calibration of $\bar{\kappa}_f$.

We simulated numerically (using the density matrix approach) the fluorescence signals averaged over longitudinal and transverse velocities, magnetic sublevels M, and spatial coordinates [see Eq. (13) in Sec. IV]. The signals S_n $(n=e,f)$ are proportional to the time integral $\int_{-\infty}^{+\infty} dt \rho_{nn}(t)$, where $\rho_{nn}(t)=P_n(t)$ is a density matrix element for state n. We have taken into account the magnetic sublevel degeneracy by considering the transition $J'' \Leftrightarrow J''+1 \Leftrightarrow J''+2$ as a set of independent three-level systems, the coupling strength of which depends on the magnetic quantum number M. This approach is valid for a linear polarization when the coupling by the laser fields is only between sublevels with the same M. In the simulation we neglect the coupling between different subsystems due to the spontaneous emission. Although the data from the simulation and the experiment do not agree perfectly, the experimentally observed trend is qualitatively well reproduced.

We observe two different trends as the detuning increases: first, a small decrease of the population flow through the final level and, second, the maximum shifts towards smaller displacements. These trends can be understood from the following considerations.

In a ladder system with strong losses from the final level f, i.e., $\Gamma_f \gg T^{-1}$, the adiabatic condition reads as[6]

$$\Gamma_f \sin 2\theta(t) \ll \sqrt{2}\Omega(t) \quad (|\Delta|=0), \tag{3}$$

$$\Gamma_f \sin 2\theta(t) \ll \frac{\Omega^2(t)}{2\Delta} \quad (|\Delta| \gg \Omega), \tag{4}$$

where $\theta(t)=\tan^{-1}[\Omega_P(t)/\Omega_S(t)]$ and $\Omega(t)=\sqrt{\Omega_P^2(t)+\Omega_S^2(t)}$. Here the Rabi frequency is defined as $\Omega_R(t)=d\varepsilon_R(t)/\hbar$ with $R=P,S$, where d is the transition dipole moment and $E_R(t)=\varepsilon_R(t)\cos(\omega_R t)$ is the electric field with amplitude $\varepsilon_R(t)$. For the present experimental conditions the detuning is comparable to the Rabi frequency, which means that this situation corresponds to an intermediate case between conditions (3) and (4). However, for $\Delta \neq 0$, a larger Rabi frequency is necessary to fulfill this condition. The point where the maximum occurs moves towards smaller negative displacements as the detuning increases. Because the Rabi frequencies of both lasers were kept to the same value, a larger overlap between the pulses is needed for achieving the maximum population flow through the final level f as the detuning is increased. The P laser controls the population dynamics because it connects the initially populated ground level to the intermediate one. This laser will pump the population faster out of the ground level if $\Delta=0$. Thus, when $|\Delta|>0$, a larger P-laser Rabi frequency will be needed. Because the Rabi frequency of the S laser must be large enough during the time while population is being transferred to level f, the displacement between the two lasers has to be smaller.

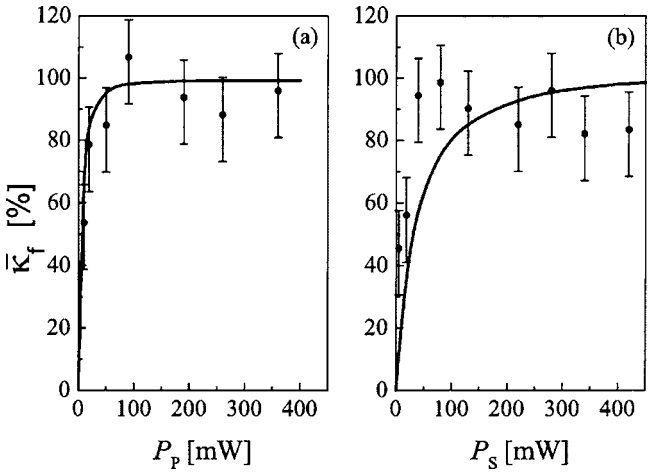

FIG. 4. Variation of the fraction $\bar{\kappa}_f$ of the initial population in level g, which is driven through level f. $\bar{\kappa}_f$ as a function of the (a) P- and (b) S-laser powers. For the data shown in (a) and (b) laser powers were kept at $P_S=420$ and P_P 320 mW, respectively. The full circles refer to the experimental data and the solid line to the numerical simulation.

B. Control through laser power

As expected for an adiabatic process, the transfer efficiency is insensitive to moderate variations of the intensity of the lasers. This feature is illustrated in Fig. 4, which shows the maximum value of the fraction $\bar{\kappa}_f$ of molecules driven through the upper level f, as a function of the P- and S-laser powers, P_P and P_S, respectively. The data of Fig. 4(a) is for a constant power $P_S=420$ mW, while P_P is varied from 10 to 360 mW. The data shown in Fig. 4(b) are obtained by varying P_S from 5 to 420 mW while $P_P=320$ mW is kept constant. For a sufficiently high power the fraction $\bar{\kappa}_f$ reaches saturation with values close to 100%. Moreover, this fraction does not decrease significantly unless the power is reduced to 50 mW or less. Within the given error bars a good agreement between theory and experiment is obtained.

The satisfaction of the adiabaticity criterion is one essential condition for driving all of the population of the initial level g through level f. In a system with strong losses the nonadiabatic coupling due to the losses will be more important than the nonadiabatic coupling produced by the time dependent Hamiltonian. A careful analysis of the population dynamics[11] shows that the following condition has to be fulfilled:

$$\bar{\Omega}_S^2 \gg \Gamma_e \Gamma_f. \tag{5}$$

Here $\bar{\Omega}_S$ is the mean value of the S-laser Rabi frequency during the relevant time interval T_{flow} of the population dynamics.

Moreover, in order to have a full depletion of the initial level population, the interaction time has to be long enough:

$$\frac{\Omega_0^2 T}{\Gamma_e} \gg 1. \tag{6}$$

Here Ω_0 is the maximum value of the P-laser Rabi frequency.

Thus, intuitively, the entire process is similar to optical pumping from the ground state directly into level f by a sufficiently strong laser S. These conditions are very well fulfilled for the highest values of the laser powers used in the present experiment. Thus, the process of driving all the populations of level g through level f benefits from the robustness of an adiabatic passage process, as does STIRAP.

C. Influence of the degeneracy

We also performed measurements using the sequence of rotational transitions $J''=1 \rightarrow J'=0 \rightarrow J=1$ for the same set of vibrational and electronic states. Because the P and S lasers are linearly polarized, this linkage represents a nondegenerate ladder of only three quantum states ($M=0$ for each level). The results were almost identical to those for the ladder $J''=7 \rightarrow J'=8 \rightarrow J=9$. Although spontaneous emission will mix M levels, this does not affect the maximum value of the population flow through the level f.

IV. THE CALIBRATION PROCEDURE

In this section, we discuss a calibration procedure which provides the quantitative information presented in Sec. III.

A. Quantifying the signal from level *f*

1. The idea

In conventional STIRAP, which operates in a Λ-coupled level scheme, the calibration of the transfer efficiency from the stable initial to the stable final level is straightforward.[8] If the system is only exposed to the P-laser radiation and if the full depletion of the population of the initial level is verified, and provided that the branching ratio for a spontaneous emission from the intermediate to the final level is known, then the fraction of the initial level which reaches the final level by optical pumping is readily determined. The enhancement of the population of the final level, when the suitably timed interaction with the Stokes laser is added, allows the determination of the transfer efficiency.

This approach is not applicable if the final level is more energetic than the intermediate level, as in a ladder system. However, also here the calibration involves a spontaneous emission. Figure 5 presents the particular levels and laser linkages needed to understand the calibration procedure.

Vibrational levels $v''>0$ in the electronic ground state carry only a very small thermal population, if any. Therefore any additional population appearing in those levels results from a spontaneous emission after the laser driven processes. The coherent laser fields drive the population from the initial level g to level f, with a coupling provided via the level e. We are interested in the decay path $f \rightarrow e_i \rightarrow g_2$, where e_i represents all the levels which contribute to the cascading transition from level f to level g_2. In our experiments we choose level g_2 in the vibrational level $v''=1$ with a rotational quantum number $J''+4$ which can receive populations by spontaneous transitions from level f, but not from level e.

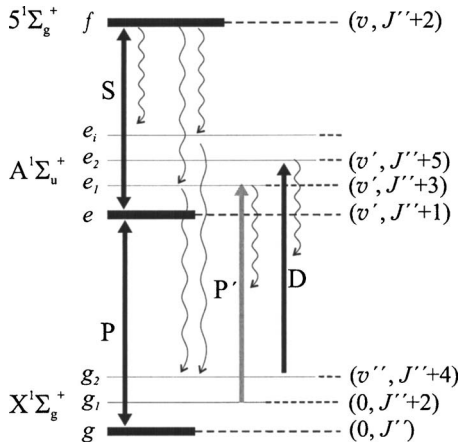

FIG. 5. Level scheme showing the couplings and various decay channels relevant for the calibration scheme.

We are interested in the fraction of the population which has flowed through level f and ends up in level g_2. This can be calculated using known transition probabilities for the sodium molecule. It means that the absolute calibration of the population of level g_2 with respect to the initial population of level g provides an absolute calibration of the population flow through level f driven by the P and S lasers.

The procedure for the calibration of the population in level g_2 is similar to the one described before for the conventional STIRAP technique in a Λ system. For this purpose, a probe laser D is used to induce fluorescence from level g_2. A small thermal population in level g_2 is needed to allow the tuning of the D-laser frequency to a transition starting from this level prior to the implementation of the transfer process of the calibration.

For an absolute calibration of the fluorescence signal we turn off the S laser and tune the frequency of P laser to resonance with the transition between levels g_1 and e_1 (laser P' in Fig. 5). The rotational numbers for these levels are $J''+2$ and $J''+3$, so spontaneous emission from level e_1 can populate level g_2 for which the rotational number takes the value $J''+4$. Using known transition probabilities, we can calculate the fraction of the population of level g_1 which is transferred to level g_2. We monitor this population by fluorescence, induced by the D laser. The ratio of two signals permits the absolute calibration of the efficiency of the population flow control.

2. The calibration signals

The signal S_e originates from a sequence of laser-induced excitations and decays that culminate in fluorescence from level e_2. The following sketch indicates the sequence of levels involved:

$$g \overset{P}{\rightarrow} e \overset{S}{\rightarrow} f \rightsquigarrow \sum_i e_i \overset{D}{\rightsquigarrow} g_2 \rightarrow e_2 \rightsquigarrow S_e. \tag{7}$$

The P- and S-laser excitations are selective. The decay from level f to various ground electronic-state levels g_i proceeds through several intermediate levels (also in other electronic

levels not shown in Fig. 5), as indicated by the summation. The D laser, acting spatially separated downstream from the S and P lasers (see Fig. 2), carries the population from a chosen one of these ground levels, g_2, into an excited level e_2. Fluorescence from this level, selected by a suitable wavelength filter, provides the signal S_e.

The molecules that contribute to the fluorescence signal have a range of longitudinal velocities $v_\parallel$ (along the molecular beam axis and hence transverse to the laser beams), of velocities $v_\perp$ along the laser beams, and of magnetic quantum numbers M, and they receive the radiation at a range of positions (x,y) within the cw laser beams. The signal S_e is the sum of fluorescences from all of these molecules. We express it as the product of several factors, appropriately summed and integrated, expressing a sequence of probabilities:

$$S_e = \eta_e \sum_i W_{f\to e_i} W_{e_i\to g_2} \int v_\parallel dv_\parallel dv_\perp dxdy \times \sum_M N_g(v_\parallel,v_\perp,x,y,M)\kappa_f(v_\parallel,v_\perp,x,y,M) \times p_D(v_\parallel,v_\perp,x,y,M). \quad (8)$$

The symbols have the following meanings.

- η_e denotes the efficiency for collecting fluorescence photons from level e_2.
- $W_{a\to b}$ is the probability that a molecule in level a (electronic, vibrational, and rotational) will undergo a transition into level b. This factor is expressible as the product of an electronic transition probability (or branching ratio) R^{elec}, a vibrational transition probability F^{FC}, and a Hoenl-London (HL) rotational transition probability F^{HL},[15]

$$W_{a\to b} = R^{\mathrm{elec}}(a,b)F^{\mathrm{FC}}(v_a,v_b)F^{\mathrm{HL}}(J_a,J_b). \quad (9)$$

  In the present expression, $\Sigma_i W_{f\to e_i} W_{e_i\to g_2}$ expresses the transition probability from f to g_2 through all possible intermediate levels.
- $N_g(v_\parallel,v_\perp,x,y,M)$ is the initial population distribution in level g. We factor this as

$$N_g(v_\parallel,v_\perp,x,y,M) = N_g^0 w(v_\perp,x,y)w(v_\parallel)w(x,y)w(M), \quad (10)$$

  where N_g^0 is the total population of state g and $w(q)$ is the distribution function over the corresponding quantity $q \equiv \{v_\parallel,v_\perp,x,y,M\}$. In our experimental conditions the geometrical size of the source of the molecular beam was much smaller than the beam diameter in the interaction region, and so $w(v_\perp,x)$ depends on spatial coordinate x.
- $\kappa_f(v_\parallel,v_\perp,x,y,M)$ is the conditional probability for a molecule to be driven into (and decay from) level f, if before the interaction with the laser fields, the molecule was in a magnetic sublevel M of the initial level g at position (x,y) with velocity components $v_\parallel$ and $v_\perp$.
- $p_D(v_\parallel,v_\perp,x,y,M)$ is the probability that a molecule in level g_2 will produce a photon via a D-laser excitation to e_2 and subsequent decay.

The calibration procedure uses an additional set of fluorescence measurements with no S-laser excitation. The D laser remains as in the first measurements, providing excitation from g_2 to e_2, but the P-laser frequency is reset to resonance with a calibration transition between one of the ground levels g_1 and excited level e_1; we refer to this as the P' laser. The sequence of excitations and decays follows the pattern shown here:

$$g_1 \xrightarrow{P'} e_1 \rightsquigarrow g_2 \xrightarrow{D} e_2 \rightsquigarrow S_c. \quad (11)$$

The sequence starting with g_2 is identical with that of sequence (7). As with the signal of Eq. (8), we express the fluorescence signal from this process as the sum and integral over several factors:

$$S_c = \eta_e W_{e_1\to g_2} \int v_\parallel dv_\parallel dv_\perp dxdy \times \sum_M \kappa_e(v_\parallel,v_\perp,x,y,M)p_D(v_\parallel,v_\perp,x,y,M) \times N_{g1}(v_\parallel,v_\perp,x,y,M). \quad (12)$$

The various factors are those defined following Eq. (8), with obvious changes of subscripts associated with the levels; like the previous $\kappa_f(v_\parallel,v_\perp,x,y,M)$ the factor $\kappa_e(v_\parallel,v_\perp,x,y,M)$ is here the conditional probability that a molecule will be excited into level e_1.

3. Calibration of averaged efficiency

Equations (8) and (12) show that, in the general case, it is impossible to extract from the ratio of the signals S_e and S_c any information about the absolute efficiency of the population flow from g to f. Obtaining a calibrated signal requires P' and D lasers that are sufficiently strong to assure that all the ground-level populations, for molecules of any velocity and location in the beam, pass out of the ground level and into the excited level e_2. Then the factors $\kappa_e(v_\parallel,v_\perp,x,y,M)$ and $p_D(v_\parallel,v_\perp,x,y,M)$ are equal to unity. This is fulfilled in our experiments because the average Doppler shift due to $v_\perp$ is smaller than the saturation width of the transitions produced by those lasers. We have verified, using an auxiliary laser downstream, that optical pumping by the P' laser fully depletes the population of level g_1. Also, under the conditions of our experiment, the size of the area seen by the detector is the same for the e- and f-level fluorescence signals.

It is not possible to examine in any detail the several contributions to the efficiency $\kappa_f(v_\parallel,v_\perp,x,y,M)$. Instead, we define an averaged efficiency

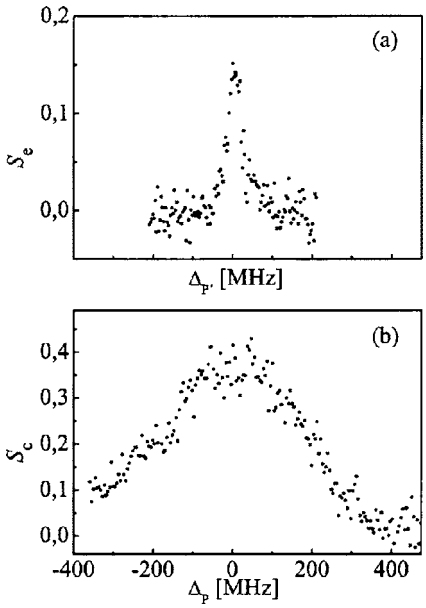

FIG. 6. Signals of laser induced fluorescence as a function of the P' and P-laser detunings $\Delta_{P'}$ and Δ_P, respectively; (a) S_e signal given by Eq. (8); (b) S_c signal as described by Eq. (12).

$$\bar{\kappa}_f = \int v_{\parallel} dv_{\parallel} dv_{\perp} dx dy \times \sum_M \kappa_f(v_{\parallel}, v_{\perp}, x, y, M) w(v_{\perp}, x, y) w(v_{\parallel}) w(x, y) w(M) \tag{13}$$

and write the signals as

$$S_e = \eta_e N_g^0 \bar{\kappa}_f \sum_i W_{f \to e_i} W_{e_i \to g_2}, \tag{14}$$

$$S_c = \eta_e N_{g_2}^0 W_{e_1 \to g_2}. \tag{15}$$

We then evaluate the averaged efficiency from the ratio of two measured signals, S_e and S_c, as

$$\bar{\kappa}_f = \frac{N_{g1}^0}{N_g^0} \frac{W_{e_1 \to g_2}}{\sum_i W_{f \to e_i} W_{e_i \to g_2}} \frac{S_e}{S_c}. \tag{16}$$

The ratio N_{g1}^0/N_g^0 is the ratio of the initial total populations of levels g_1 and g. This ratio is known from the diagnostics of the molecular beam. For small J the thermal distribution is typically characterized by a rotational temperature $T_{\mathrm{rot}} \approx 40$ K resulting in a ratio of the populations $N_{g1}^0/N_g^0 = 0.96$. The ratio of the various transition probabilities W, as expressed in Eq. (16), is equal to 1.93. This value is obtained as explained below.

Level f of the $5\ ^1\Sigma_g^+$ electronic state decays to the intermediate electronic states $A\ ^1\Sigma_u^+$, $2\ ^1\Sigma_u^+$, $B\ ^1\Pi_u$, $2\ ^1\Pi_u$, and $3\ ^1\Sigma_u^+$. From a standard quantum chemistry approach based on pseudopotentials for an atomic core representation,[14] the branching ratio of the decay to the $A\ ^1\Sigma_u^+$ was estimated to be near 80% and that of the $2\ ^1\Sigma_u^+$ state to around 20%. Furthermore, the $2\ ^1\Sigma_u^+$ state can also decay to the $2\ ^1\Sigma_g^+$ and $B\ ^1\Pi_g$ states (which do not decay on the time scale relevant for our experiment). Taking these additional channels into account, we concluded that no more than 10% of the population in the $2\ ^1\Sigma_u^+$ state can decay to the electronic ground state $X\ ^1\Sigma_g^+$. Thus, the fact that we have taken into account only a single electronic decay path (through the $A\ ^1\Sigma_u^+$ state) for the calibration procedure gives us an upper limit of the value of the average efficiency, with an accuracy of 10%. This systematic deviation is included in the error bars of the experimental data presented in Sec. III, together with the statistical error for the determination of the signals S_c and S_c. The contribution of the statistical error is symmetric with respect to the calculated values of $\bar{\kappa}_f$. The systematic and statistical errors combine to deviations of +12% and −15% (see Figs. 3 and 4). From a previous experimental work[13] we had concluded that only about 35% of the population from level f decays through the $A\ ^1\Sigma_u^+$ state. A new analysis of those data, now based on extensive numerical simulation studies,[15] has confirmed a branching ratio near 80%.

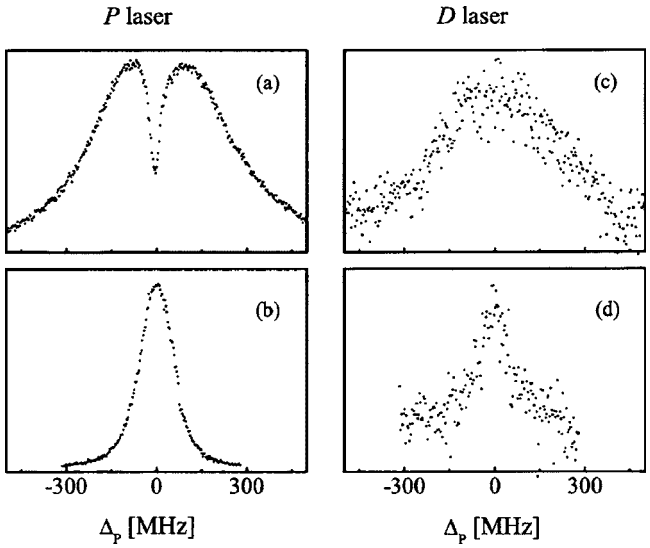

FIG. 7. Variation of the fluorescence signals (in arbitrary units) induced by the P [(a) and (b)] and the D [(c) and (d)] lasers as a function of the P-laser detuning Δ_P. The P-laser power was 260 mW for the upper frames [(a) and (c)] and 4.5 mW for the lower ones [(b) and (d)].

Figure 6 displays the two signals S_c and S_e to be compared. These two signals are generated as the P and P' laser frequencies are scanned across the resonance with the g-e transition. The D-laser frequency is kept fixed, and the fluorescence induced by this laser produces both S_c and S_e. The S_c signal has a broader width (in comparison with S_e) and exhibits the typical plateau around the resonance. This shape arises from the fact that the P and P' laser intensities are high enough to saturate their respective transition on and near the resonance. The S_e signal, however, corresponds to the two-photon process explained in the section above, thus exhibiting a narrower line width. The ratio of the maxima of S_e and S_c is used in Eq. (16).

B. Comments on the signal from level *e*

The detection geometry used in the present experiments needs to be carefully considered. Because some consequences may be easily overlooked[16] we show and discuss in this section the data presented in Fig. 7. We provide a direct

proof that the origin of the doublet-type structure[16] is geometric. In particular, we discuss the consequences of optical pumping which, combined with the actual detector geometry, prevent a reliable quantitative calibration of the signal from level e.

The magnitude of any laser induced fluorescence signal will be affected by optical pumping if the excitation probability approaches unity and the spatial region, from which fluorescence is collected does not cover the entire laser beam profiles. In the present experiment, the fluorescence from level f is collected by a fiber bundle with an aperture of 2×5 mm^2 (with the long axis aligned parallel to the molecular beam axis), which is large compared to the laser beam diameter. However, the fluorescence from level e is collected by a single fiber with a core diameter of 200 μm, which is smaller than the laser beam diameter. Thus, the detection channel for the f-level fluorescence collects light across the entire laser beam profiles with about uniform efficiency, but the detection of the e-level fluorescence is restricted to the region near the P-laser beam axis. The fluorescence signals are imaged onto the end surface (bundle) or core (single) of the fiber using a single lens without magnification.

We discuss the consequences of the difference in the detection geometry by considering a trajectory $x(t)$ of a molecule through the laser beam, subject to an intensity dependent (and thus spatially varying) probability density $p_{\mathrm{ex}}[I_P(x)]$ (cm^{-1}) for being excited and the probability

$$P_{\mathrm{ex}} = \int p_{\mathrm{ex}}[I_P(x)]dx, \tag{17}$$

for a molecule to be excited after completion of the transit through the P-laser beam. We, furthermore, note that the electronic lifetime is short compared to the transit time through the laser beam. Thus, the fluorescence intensity originating from a given location x is proportional to the laser intensity $I_P(x)$ at that location.

If P_{ex} is small (either because the P-laser intensity is small or the P-laser frequency is tuned far off resonance), the spatial variation of the fluorescence intensity is proportional to p_{ex} which in turn is proportional to the local P-laser intensity $I_P(x)$. Thus, the fluorescence intensity will be maximal near the region close to the P-laser beam axis. When P_{ex} increases, the flux of molecules in level g, which reaches the laser beam axis, decreases because a substantial fraction of those molecules are already excited in the spatial wing of the laser beam profile and have decayed to other levels (for instance to level g_1). If P_{ex} approaches unity, most molecules are excited in the wing of the laser beam profile and only few reach the region near the beam axis where they could be detected.

Figure 7 shows spectral profiles of the e-level fluorescence induced by the P laser from molecules in level g, while the S laser is switched off. In Fig. 7(a) the power is set at a level where P_{ex} is close to unity when the P-laser frequency is tuned to resonance with the g-e transition. The excitation probability decreases with the increasing detuning Δ_P from the resonance. Thus for the on-resonance tuning only few molecules will reach the center of the laser beam which is seen by the detector, and the observed signal is small. With the increasing detuning from resonance, the signal increases since more molecules in level g reach the laser beam axis despite the fact that P_{ex} decreases. Therefore a dip is observed in the central part of the profile for $\Delta_P=0$. When the laser power is reduced to a level such that $P_{\mathrm{ex}} \ll 1$, the flux of molecules which reach the P-laser beam axis in level g does not change appreciably as Δ_P is varied, and thus a dip is not observed [see Fig. 7(b)].

A direct proof of the fact that the profile shown in Fig. 7(a) is indeed caused by optical pumping and the resulting change of location from where most of the fluorescence originates is given in Figs. 7(c) and 7(d). These figures show the fluorescence induced by laser D from level g_1 downstream from the interaction region with the P laser. Level g_1 is populated by fluorescence from level e after the excitation of level g by the P laser (see Fig. 5). The fluorescence signal is proportional to the flux of molecules in level g_1 through laser beam D. This flux, in turn, is proportional to P_{ex} and is not sensitive to the spatial variation of the excitation probability within the P-laser beam profile.

V. CONCLUSIONS

We have implemented and demonstrated a method which allows an efficient control of the population flow through different levels in a ladder system. This control is done by changing the delay between the pulses. For a counterintuitive pulse sequence, the S pulse precedes the P pulse, and the population flow through level f is maximal. We explored the limits of this technique by studying the influence of laser powers and detunings. In addition, we have presented an approach to the calibration of the efficiency of the population flow through the upper level. This method is based on knowledge of the rich variety of rovibrational transitions in molecular systems and is independent of the kind of stepwise excitation scheme used. Finally, we have analyzed the consequences of the detection geometry and show why optical pumping may lead to a distortion of the line shape.

ACKNOWLEDGMENTS

One of the authors (R.G.F.) acknowledges support by the EU through the research training network QUACS (HPRN-CT-2002-0309). Another author (L.P.Y.) acknowledges support by the Deutsche Forschungsgemeinschaft through (436-UKR-113/6). Two authors (B.W.S. and L.P.Y.) acknowledge support through funds from the Max-Planck Forschungspreis 2003. Another author (A.E.) acknowledges the support by the EU TOK project LAMOL (MTKD-CT-2004-014228), European Social Fund, Latvian Science Council, and NATO Grant No. EAP.RIG.981387. The authors thank Olivier Dulieu for providing his theoretical results about radiative decay properties prior to publication.

[1] H.-G. Rubahn and K. Bergmann, Annu. Rev. Phys. Chem. **41**, 735 (1990).
[2] M. Shapiro and P. Brumer, *Principles of the Quantum Control of Molecular Processes* (Wiley, New York, 2003); S. A. Rice and M. Zhao, *Optical Control of Molecular Dynamics* (Wiley Interscience, New York, 2000).
[3] A. Ekert and R. Jozsa, Rev. Mod. Phys. **78**, 733 (1996).

[4] T. F. Gallagher, *Rydberg Atoms* (Cambridge University Press, Cambridge, 1994).
[5] A. M. F. Lau, Phys. Rev. A **14**, 279 (1976); J. Wong, J. C. Garrison, and T. H. Einwohner, *ibid.* **16**, 213 (1977).
[6] R. Garcia-Fernandez, A. Ekers, L. P. Yatsenko, N. V. Vitanov, and K. Bergmann, Phys. Rev. Lett. **95**, 043001 (2005).
[7] N. V. Vitanov, T. Halfmann, B. W. Shore, and K. Bergmann, Annu. Rev. Phys. Chem. **52**, 763 (2001).
[8] U. Gaubatz, P. Rudecki, S. Schiemann, and K. Bergmann, J. Chem. Phys. **92**, 5363 (1990); K. Bergmann, H. Theuer, and B. W. Shore, Rev. Mod. Phys. **70**, 1003 (1998); N. V. Vitanov, M. Fleischhauer, B. W. Shore, and K. Bergmann, in *Advances in Atomic Molecular and Optical Physics*, edited by B. Bederson and H. Walther (Academic, New York, 2001), Vol. 46, pp. 55. (Wiley, New York, 1990).
[9] B. Sueptiz, B. C. Duncan, and P. L. Gould, J. Opt. Soc. Am. B **14**, 1001 (1997).
[10] H. A. Camp, M. H. Shah, M. L. Trachy, O. L. Weaver, and B. D. DePaola, Phys. Rev. A **71**, 053401 (2005).
[11] L. P. Yatsenko, A. A. Rangelov, N. V. Vitanov, and B. W. Shore, J. Chem. Phys. **125**, 014302 (2006), following paper.
[12] E. Arimondo and G. Orriols, Nuevo Cimento **17**, 333 (1976); G. Alzetta, A. Gozzini, L. Moi, and G. Orriols, Nuovo Cimento Soc. Ital. Fis., B **36**, 5 (1976).
[13] R. Garcia-Fernandez, A. Ekers, J. Klavins, L. P. Yatsenko, N. N. Bezuglov, B. W. Shore, and K. Bergmann, Phys. Rev. A **71**, 023401 (2005).
[14] Olivier Dulieu (private communication).
[15] R. Garcia-Fernandez, A. Ekers, N. N. Bezuglov, L. P. Yatsenko, O. Dulieu, M. Ayrnar, B. W. Shore, and K. Bergmann, J. Chem. Phys. (in preparation).
[16] K. Bergmann and E. Gottwald, Chem. Phys. Lett. **78**, 515 (1981).